Biophysical Chemistry 29 (1988) 63–76
Elsevier

BPC 01214

Time-resolved optical spectroscopy and structural dynamics following photodissociation of carbonmonoxyhemoglobin

Lionel P. Murray, James Hofrichter, Eric R. Henry and William A. Eaton

Laboratory of Chemical Physics, National Institute of Diabetes and Digestive and Kidney Diseases, National Institutes of Health, Bethesda, MD 20892, U.S.A.

Accepted 15 October 1987

Hemoglobin; Photodissociation; Time-resolved optical spectroscopy; Ligand-binding kinetics; Structural dynamics

A summary is presented of our current understanding of the kinetics of ligand rebinding and conformational changes at room temperature following photodissociation of the carbon monoxide complex of hemoglobin with pulsed lasers. The events which occur subsequent to excitation have been followed over 12 decades in time, from about 100 fs to the completion of ligand rebinding at about 100 ms. Experiments with picosecond and subpicosecond lasers by others, together with molecular dynamics simulations, indicate that by 1 ns the deoxyhemoglobin photoproduct is in a thermally equilibrated ground electronic state, so that subsequent processes are unaffected by the initial laser excitation. The principal results have been obtained from time-resolved optical absorption spectroscopy using a sensitive nanosecond laser spectrometer. Five relaxations have been observed which are interpreted as geminate rebinding at about 50 ns that competes with motion of the ligand away from the heme which produces a tertiary conformational change, a second tertiary conformational change at 0.5–1 μs, transition from the R to T quaternary structure at about 20 μs, and overall bimolecular rebinding of ligands from the solvent to the R and T quaternary structures at about 200 μs and 10 ms. Assuming that the dissociation pathway in photolysis experiments is the reverse of the association pathway, we find that for the R state there is a 40% probability that the ligand will bind to the heme after entering the protein, and a 60% probability that it will return to the solvent. Studies on the α-subunit of an iron-cobalt hybrid hemoglobin indicate that carbon monoxide enters the protein at the same rate for both R and T quaternary structures. For the α-subunit in the T state the probability of binding after entry is much lower, and the ligand returns to the solvent more than 99% of the time, accounting for the 60-fold overall lower association rate. This decreased probability of binding results from a decreased rate of binding to the heme from within the protein, and not an increased rate of return to the solvent. There are still unresolved problems on the basic structural description of carbon monoxide binding and dissociation, particularly the functional significance of the tertiary relaxations in both the R and T states, and the precise number of kinetic barriers within the protein.

1. Introduction

Dissociation of ligands from hemoglobin is a multistep process [1]. This has been demonstrated by experiments in which a short laser pulse is used to break the heme-ligand bond. Not all photodissociated ligands escape from the protein into the solvent. A certain fraction rebind from within the protein. This process is called geminate recombination. At room temperature geminate recombination of carbon monoxide occurs on a nanosecond time scale [2–18], while for oxygen geminate rebinding is observed on both nanosecond [8,9,19,20] and picosecond time scales [2,3,10,21,22]. A structural basis for geminate recombination has been known since the early X-ray findings that there is no open path from the heme iron to the solvent [23,24]. Residues on the surface of the protein would have to be displaced to allow the ligand to leave the protein after dissociation of the iron-ligand bond, or to enter the protein from the

Correspondence address: W.A. Eaton, Laboratory of Chemical Physics, Building 2, Room B1-04, National Institute of Diabetes and Digestive and Kidney Diseases, National Institutes of Health, Bethesda, MD 20892, U.S.A.

solvent. In terms of kinetics, this displacement introduces a free energy barrier for both the entry and the exit of the ligand.

In addition to geminate recombination, pulsed laser measurements have exposed a series of time-dependent changes in both the optical absorption [14,15,18,25,26] and resonance Raman spectra [27–34] of the deoxyheme photoproduct. Spectroscopic changes of the deoxyheme are expected from X-ray crystallographic studies. Comparison of the X-ray structures of liganded and deoxyhemoglobin in both the R and T quaternary structure shows changes that might be observable by time-resolved spectroscopy [35–38]. These include displacement of the iron from the heme plane and a doming of the porphyrin, a reorientation of the heme plane [39–41], and tilting of the proximal histidine relative to the heme plane as a result of motion of the F-helix. The interpretation of spectral changes in terms of specific structural changes is still a major problem in making detailed interpretations of the results of both time-resolved absorption and resonance Raman studies. Molecular dynamics calculations are, however, beginning to play a significant role in the interpretation of experimental results on a subnanosecond time scale [42,43].

In this article we summarize the major results of our studies on the kinetics of conformational changes and ligand rebinding in human hemoglobin following photodissociation of the carbon monoxide complex at room temperature. The principal objectives of this work have been to develop a mechanism for ligand dissociation and binding that describes the functional role of the various conformational changes and to determine the elementary kinetic steps of this mechanism that are responsible for kinetic cooperativity [14,18,44]. Our approach has been to make very precise measurements of optical absorption spectra at various time delays following the photodissociation of the carbon monoxide complex with nanosecond laser pulses [14,15,18,44]. From these measurements we have been able to determine the kinetics of spectral changes resulting from conformational changes in the deoxy photoproduct, as well as the much larger spectral changes due to ligand rebinding. In addition to the experimental studies, we have employed molecular dynamics calculations to simulate the photodissociation process [42,43]. These calculations have been used as a guide to understanding events that occur on a subnanosecond time scale.

We begin by briefly summarizing the results of these calculations and some of the experimental results from other laboratories using picosecond and subpicosecond lasers.

2. Subnanosecond experiments and molecular dynamics simulations

To understand fully the results of our studies with nanosecond lasers, it is important to consider first what processes have already taken place. One would like to know as much as possible about the details of the photodissociation process in order to determine the relation between photodissociation and the spontaneous thermal dissociation of the ligand. Important results have been obtained both from experiments using subnanosecond laser pulses and from molecular dynamics simulations of the photodissociation process.

The mechanism of photodissociation is still not clear. Spectroscopic studies employing polarized single-crystal absorption, and natural and magnetic-field-induced circular dichroism of solutions, together with molecular orbital and crystal field calculations, have provided a general description of the nature of the electronic transitions that give rise to the observed optical spectrum of the heme-CO complex [41,45,46]. The lowest observed states arise from electronic promotions within the iron d orbitals [46]. There are several low-lying excited states of the heme-CO complex with zero, two, or four unpaired electrons [3,41,46] which might be expected to have a repulsive potential for CO binding because there is an electron in the d_{z^2} orbital which is antibonding for the axial ligands [47,48]. Any one of these could lead to photodissociation [3,48]. The simplest description of the photophysics would be one in which optical excitation into the porphyrin $\pi \rightarrow \pi^*$ state is followed by relaxation into the $d \rightarrow d$ excited state with four unpaired electrons, which has the same d-orbital electronic configuration as the deoxyheme

ground state ($d^2_{xz}d_{xy}d_{yz}d_{z^2}d_{x^2-y^2}$) [46,49]. In this description photodissociation occurs on a single potential surface. After correcting the steady-state quantum yield for geminate recombination, the photochemical quantum yield for myoglobin is very close to unity [50].

Experiments on carbonmonoxyhemoglobin with 250 fs pulses show that the ground-state absorption spectrum in the region of the intense porphyrin $\pi \rightarrow \pi^*$ transition disappears in a time shorter than the pulse width [51,52]. The appearance of a deoxyheme-like absorption spectrum is slower, with a time constant of about 300 fs. This result was interpreted as indicating that a deoxyheme in its ground electronic state with the iron displaced from the heme plane is formed within about 300 fs. Molecular dynamics studies support this interpretation. Calculations have been performed on a complete α-subunit of hemoglobin in vacuo [42]. (The absence of solvent in this calculation should not have a major effect on the result since the heme is well buried inside the protein.) In order to simulate the photolysis event, a trajectory of the liganded molecule was interrupted, the iron-carbon monoxide bond was broken by introducing a weakly repulsive potential, and the potential function describing the iron-porphyrin and iron-histidine bonding was changed to one appropriate for a deoxyheme in its ground electronic state. These calculations show that the iron can be displaced from the heme plane to a position close to that found in deoxyhemoglobin in less than 150 fs, in agreement with the interpretation of the optical study (fig. 1). The trajectories are not sufficiently accurate, however, to determine the extent of the displacement to better than ± 0.1–0.2 Å. Moreover, time-resolved resonance Raman studies of the 'core-size marker band' suggest that the iron displacement at 30 ps following photolysis is smaller than that found in equilibrium deoxyhemoglobin until the time regime 10–300 ns [27–29,53].

A major difference between photodissociation and thermal dissociation is that there is a large amount of excess energy deposited in the heme as a result of absorption of one or more photons. For absorption of a single photon this energy is the difference between the photon energy (e.g., 54 kcal/mol for a 530 nm photon) and the bond dissociation energy (about 20 kcal/mol) or about 35 kcal/mol. In a typical experiment with picosecond pulses many photons are absorbed per heme (20 per heme in the original study [3]). If this energy is converted into excess vibrational energy of the ground electronic state of the deoxyheme photoproduct, the resulting temperature of the heme can be many hundreds of degrees above the ambient temperature [43,54]. Conversion of a single 530 nm photon into excess vibrational energy of a metal porphin is estimated to raise the temperature by about 460 K [43].

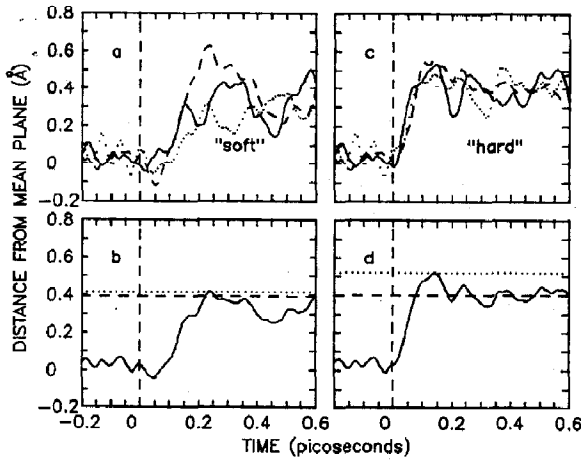

Fig. 1. Photodissociation of HbCO α-subunit of hemoglobin (from ref. 42). The distance of the iron from the mean plane of the pyrrole nitrogens for three trajectories is plotted as a function of time using two different deoxyheme potential functions (a and c). The vertical dashed line indicates the time at which the heme potential function was changed to simulate the initiation of photodissociation of the carbon monoxide ligand. The curves in (b and d) are the average displacements calculated from the three curves in (a and c). The horizontal dashed lines in (b and d) are the displacements obtained from a 9 ps average starting at +1 ps, while the horizontal dotted line is the average displacement from a deoxyhemoglobin trajectory.

To determine how fast the heme gives up this excess vibrational energy to the surrounding protein, i.e., how fast the heme 'cools', a molecular dynamics simulation was performed [43]. In these calculations the velocities of the 24 porphyrin skeletal atoms, the atoms of the π electron chromophore, were scaled to increase the kinetic en-

ergy by amounts corresponding to typical photon energies in photolysis experiments. The temperature of the heme was calculated from the average kinetic energy of the atoms. Calculations on myoglobin and cytochrome *c* give very similar results, with about 50% of the temperature decrease occurring in about 10 ps (fig. 2). The energy is transferred to the protein by collisions between the heme and protein atoms. Analysis of the temperature of the protein atoms indicates that they heat up relatively uniformly, suggesting that the energy is taken up by low-frequency modes that involve collective motions of a large number of atoms [55,56]. By 50 ps the temperatures of both the heme and the protein are stable. It will be interesting to include solvent in future calculations to simulate the complete thermal equilibration of the protein. Approximate classical heat conduction calculations suggest that the protein atoms thermally equilibrate with the solvent in less than 100 ps.

Experiments with 8-ps pulses are consistent with the molecular dynamics simulations. Spectral changes of the myoglobin deoxy photoproduct are observed that relax in 10–50 ps to a spectrum that is stable until 1 ns [57]. Similar results would be expected for hemoglobin. These spectral changes could correspond to decay of electronically excited states [2,51,52,57,58], or, as suggested by the molecular dynamics simulations, to the dissipation of excess vibrational energy resulting from laser heating [43]. Not only is the shape of the optical spectrum of the hemoglobin deoxy photoproduct stable from about 30 ps to 10 ns, but no amplitude changes have been observed, indicating that there is less than about 10% subnanosecond geminate rebinding at room temperature [3,10,59]. In addition to optical absorption measurements, resonance Raman experiments have also been performed in the time regime 30 ps–10 ns. Both the iron-histidine stretching frequency [33] and the porphyrin core size marker band have been monitored [27–29,53]. Although there are shifts in these bands relative to their frequencies in equilibrium deoxyhemoglobin, there are no changes between 30 ps and 10 ns.

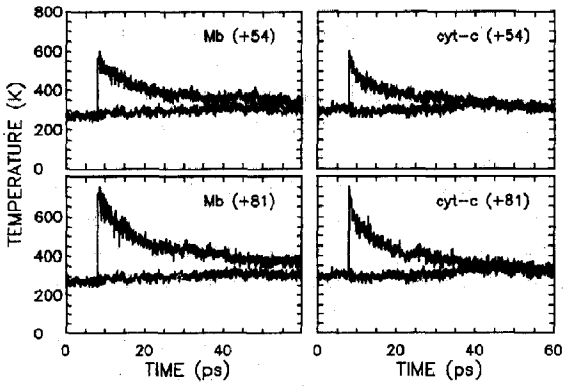

Fig. 2. Molecular dynamics simulation of cooling after laser excitation for absorption of a 353 nm (81 kcal/mol) or 530 nm (54 kcal/mol) photon by myoglobin and cytochrome *c* (from ref. 43). The kinetic temperature of the 24 porphin skeletal atoms (the π-electron chromophore), obtained from the average of eight trajectories, is plotted vs. time.

The net result of the subnanosecond experiments and molecular dynamics simulations is that in less than 1 ns photodissociation of the carbon monoxide complex of hemoglobin produces a molecule at a temperature which is close to ambient with the iron already displaced from the heme plane, but possibly not as far as in equilibrium deoxyhemoglobin. Furthermore, there does not seem to be any reason at present to believe that there are significant differences between the photodissociated molecule and the spontaneously dissociated molecule for times of nanoseconds or longer. With this background we can proceed to discuss the results of our photodissociation experiments with nanosecond laser pulses.

3. Kinetics of conformational changes and ligand rebinding to R state hemoglobin

The simplest and most useful framework for discussing the results of laser-photolysis experiments is the two-state allosteric model [35,44, 60–63]. According to this model hemoglobin exists in only two affinity states, a low-affinity T state having the quaternary structure of the fully deoxy molecule and a high affinity R state with the quaternary structure of the fully liganded molecule. Ligand binding to the heme in a T state molecule produces conformational changes that are transmitted to the intersubunit interface be-

tween the $\alpha\beta$ dimers that are related by a 2-fold axis. This interface becomes increasingly destabilized as successive ligands bind and, after the binding of two or three ligands, is sufficiently destabilized to tip the equilibrium between the two quaternary conformations in favor of the R state, causing a 'switch' from T to R. An essential feature of the model is that within each quaternary structure the binding constant for a heme does not change with the number of ligands bound, but depends only on the quaternary structure. There are, then, two dissociation and rebinding mechanisms to be investigated, one in which the liganded molecules are in the R state prior to photodissociation, and another in which they are in the T state prior to photodissociation. We shall see that it is possible to explain all of the observed kinetic behavior in the photolysis experiments without having to introduce a more complex model. We first discuss the results on hemoglobin in which all molecules are in the R quaternary structure prior to photodissociation.

One problem with measurements on the intact tetramer is that the spectra of the α and β hemes are almost identical, so that it is not possible to study the behavior of the individual subunits. This problem can be overcome by working with iron-cobalt hybrid hemoglobins in which cobalt is substituted for iron in either the α- or β-subunit [64]. These molecules have several important properties [19,20,64–66]. Cobalt porphyrins do not bind carbon monoxide at all. Hemoglobin in which cobalt is substituted for iron in both α- and β-subunits has a structure that is unchanged from the all-iron molecule [67], and exhibits only slightly reduced cooperativity in oxygen binding [68]. It is therefore possible to treat the hybrid molecules, $\alpha(\text{Fe-CO})_2\beta(\text{Co})_2$ and $\alpha(\text{Co})_2\beta(\text{Fe-CO})_2$, as though they are doubly liganded intermediates of normal all-iron hemoglobin.

Fig. 3 shows a portion of the data from a typical experiment on intact carbonmonoxyhemoglobin. There is a multiphasic decrease in the amplitude of the spectrum due to ligand rebinding. There is also a change in the shape of the spectrum, due to conformational changes in the deoxy photoproduct. To condense and filter the information contained in the approx. 100 mea-

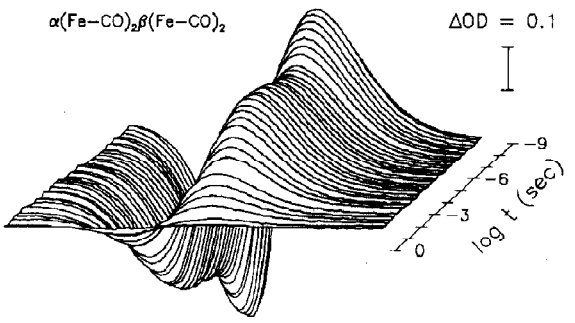

Fig. 3. Transient spectra (400–460 nm) as a function of the logarithm of time following complete photodissociation of carbonmonoxyhemoglobin at room temperature in 0.1 M potassium phosphate buffer, pH 7.0 (from ref. 15).

sured spectra the data are subjected to singular value decomposition [14,15,69]. This analysis decomposes the observed spectra into a set of orthonormal basis spectra, together with the time courses of the amplitudes of the basis spectra. After fitting the time courses with a sum of exponentials we obtain a ligand rebinding curve as well as the spectral changes associated with each of the observed relaxations.

Fig. 4 shows the results of the analysis of the data in fig. 3. Five relaxations are invariably observed, which we label I–V. The spectral changes in each relaxation appear to be almost exclusively changes in the spectrum of the deoxy photoproduct, and consist mainly of an increase of the deoxyheme absorption intensity with time. By varying the carbon monoxide pressure and the degree of photolysis it has been possible to assign four out of the five relaxations to well-defined molecular processes [14,44]. About 40% of the hemes rebind carbon monoxide in relaxation I at about 50 ns. Experiments on the iron-cobalt hybrid molecules indicate that the geminate yield and relaxation times are very similar for the α- and β-subunits [15,18]. Decreasing the carbon monoxide pressure by 10-fold has no effect on either the amplitude or time constant for rebinding, indicating that it is a unimolecular process and therefore corresponds to geminate rebinding [14]. In partial photolysis experiments, where the immediate photoproduct contains two or three liganded hemes, the amplitude and rate for relaxa-

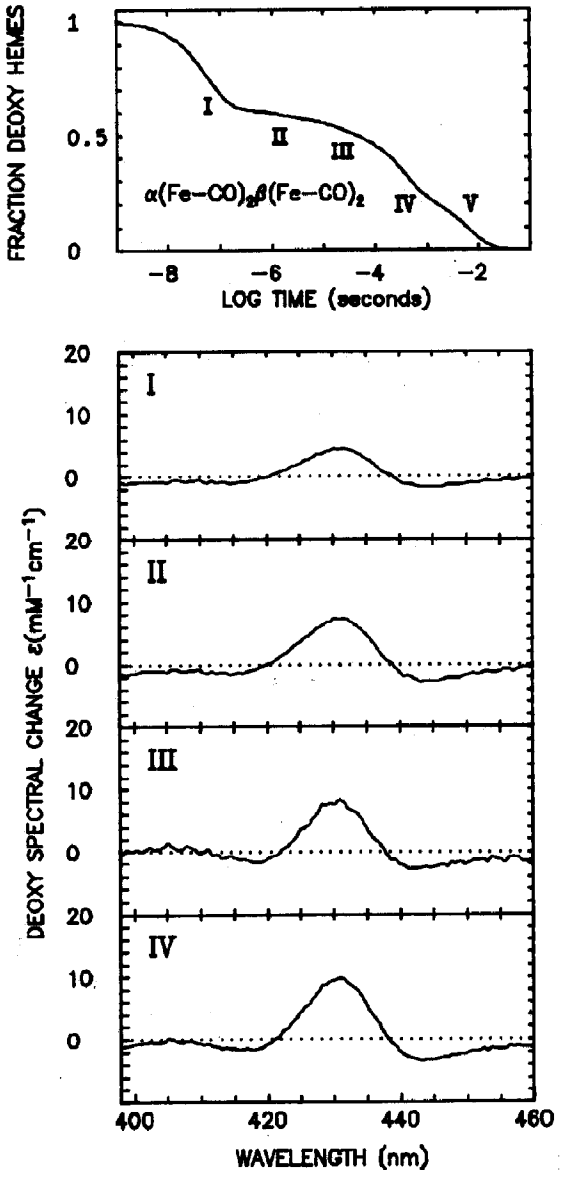

Fig. 4. Ligand rebinding curve and spectral changes associated with each relaxation following complete photodissociation of carbonmonoxyhemoglobin, calculated from the data in fig. 3 (from ref. 15).

tion I are unchanged [14]. This is consistent with an allosteric picture in which the kinetic properties, at least for the first 100 ns or so after photodissociation, do not depend on the number of bound ligand molecules per se, but only on the quaternary structure.

There is also a deoxyheme spectral change associated with the geminate rebinding in relaxation I. The rate of this spectral change is indistinguishable from the rate of geminate rebinding under a variety of solution conditions [14,15,18]. This result indicates that the spectral change reflects a parallel process that competes with geminate rebinding, and is not some unrelated process. The observed rate for relaxation I, then, is the sum of the rates for geminate rebinding and the process that causes the spectral change in the deoxy molecule. * We shall discuss possible structural interpretations of this spectral change later.

Relaxation II at 0.5–1 μs is the most difficult to interpret. It consists mainly of a spectral change of the deoxy heme, with barely detectable geminate rebinding. In our initial studies [14,44], there was a hint that the extent of rebinding may depend on the carbon monoxide pressure, but subsequent studies revealed no significant pressure dependence (J. Hofrichter, unpublished results).

Relaxation III at 20 μs corresponds to the quaternary transition from R to T. This interpretation is based mainly on the results of partial photolysis experiments [14]. If the degree of photolysis is sufficiently low, the photoproduct consists almost completely of molecules with three ligands bound. Three-fold liganded molecules are prevented thermodynamically from switching to the T quaternary structure, so that there should be no observable R → T transition. This is indeed what is observed. In experiments discussed later, where the liganded molecule is already in the T conformation prior to photodissociation, this relaxation is absent, confirming the assignment from a totally different approach [18].

Relaxations IV and V at about 200 μs and about 10 ms are assigned on the basis of previous kinetic studies as bimolecular rebinding to hemoglobin in the R and T quaternary conformations.

* For parallel first-order processes with a common reactant (in this case the immediate photoproduct), the observed relaxation rate is the sum of the rates for the individual processes, and the fraction of each process is given by the rate constant for the individual process divided by the observed relaxation rate.

The basis for this interpretation is that in partial photolysis experiments only a rapid (200 μs) bimolecular phase is observed; in full photolysis experiments, where the slower bimolecular phase is observed, the rate for the slow phase is close to the rate observed when fully deoxygenated hemoglobin is mixed with carbon monoxide [14,70].

There is additional information about R → T switching rates in the amplitudes of the R and T state bimolecular rebinding phases. In a two-state model the fraction of hemes that bind with a T state overall association rate after photodissociation of an R state molecule is the fraction of deoxy subunits which belong to tetramers that change quaternary structure from R to T. If only zero-liganded tetramers switch, the fraction of hemes that bind with a T state rate is $(1-\phi)^4$ for all-iron hemoglobin, and $(1-\phi)^2$ for the iron-cobalt hybrids (where ϕ is the total geminate yield), minus the fraction of hemes that bind during the $R_0 \rightarrow T_0$ transition (relaxation III). This simple relation is realized for the iron-cobalt hybrids, indicating that the $R_1 \rightarrow T_1$ rate is slower than the R state binding rate (1/240 μs for $\alpha(Co)_2\beta(Fe)\beta(Fe\text{-}CO)$ in phosphate buffer [15], and 1/150 μs for $\alpha(Fe)\alpha(Fe\text{-}CO)\beta(Co)_2$ in bis-tris buffer [18]). For all-iron hemoglobin the fraction of hemes binding with a T state rate is more than twice that predicted from only $R_0 \rightarrow T_0$ switching, indicating that the $R_1 \rightarrow T_1$ rate is comparable to the overall association rate for the R state (1/200 μs) [14].

4. Kinetics of conformational changes and ligand rebinding to T state hemoglobin

Obtaining the equivalent kinetic information on molecules that are in the T quaternary structure prior to photolysis presents special problems. One possibility is simply to reduce the fractional saturation of the sample to close to zero thereby producing a population of partially liganded T state molecules. This idea fails because as the fraction of the liganded R state molecules decreases, their dilution increases dissociation into dimers with the result that a significant liganded dimer population is present at any practically useful hemoglobin concentration [71,72]. It is possible, however, to use allosteric effectors to switch the doubly liganded iron-cobalt hybrid, α(Fe-

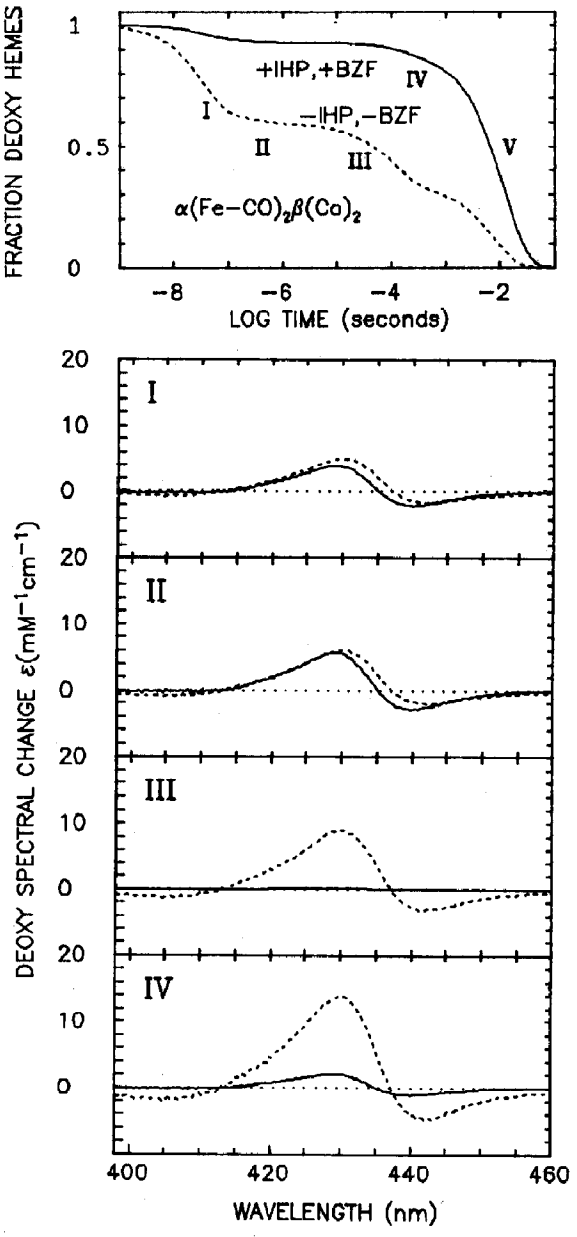

Fig. 5. Ligand rebinding curve and spectral changes following complete photodissociation of the iron-cobalt hybrid hemoglobin $\alpha(Fe\text{-}CO)_2\beta(Co)_2$ in the R (dashed curves) and T (solid curves) quaternary conformations at room temperature (from ref. 18).

$CO)_2\beta(Co)_2$, almost completely into the T state [65]. The hybrid $\alpha(Co)_2\beta(Fe\text{-}CO)_2$ remains in the R state in the presence of allosteric effectors [65,66].

Fig. 5 compares the results for photodissociation of $\alpha(Fe\text{-}CO)_2\beta(Co)_2$ in the presence and absence of the allosteric effectors inositol hexaphosphate (IHP) and bezafibrate (BZF) [18]. IHP binds in the cleft between the β-subunits [73], while BZF binds in that between the α-subunits [74]. In the absence of allosteric effectors this molecule behaves like R state hemoglobin. The addition of IHP and BZF produces striking changes in the amplitudes of the ligand rebinding phases. There is a marked reduction in the fraction of hemes that undergo geminate recombination and rapid bimolecular rebinding (relaxation IV). Over 90% of the ligand rebinding takes place in the slow bimolecular phase (relaxation V) characteristic of T state rebinding. In spite of these large amplitude changes, there is almost no change in the observed relaxation time for geminate rebinding, bimolecular rebinding to the R state, or bimolecular rebinding to the T state. The molecule appears to behave like an ideal two-state allosteric molecule. The only influence of the allosteric effectors is to increase the population of the T state molecules relative to that of the R state, without affecting the kinetic properties of either quaternary state.

A small amount of rapid bimolecular rebinding (relaxation IV) remains, indicating that conversion of the population to the T state is incomplete. To obtain the properties of the pure T state the various kinetic properties can be extrapolated to zero rapid bimolecular rebinding, i.e., to conditions where there are no R state molecules and no dimers (which have a bimolecular rate very similar to that of the R state). As pointed out earlier, this extrapolation results in zero amplitude for the spectral change in relaxation III, which is consistent with its assignment to the $R \rightarrow T$ transition. * The extrapolated value for the geminate yield in relaxation I is -0.009 ± 0.009. The geminate yield cannot, of course, be zero since there must be some finite probability of rebinding to the heme after photodissociation. (If the intermediate produced by photodissociation is the same as that obtained after the ligand enters the protein from the solvent, then the geminate yield must be a finite, positive number otherwise no reaction would take place). For the present we use a value of 0.01 as an upper limit for the geminate yield of the T state molecule [18].

In order to complete the kinetic analysis of geminate rebinding in the T state we need to know the rate for relaxation I. Determination of the relaxation rate from the ligand rebinding progress curve is not possible because the observed amplitude is dominated by the R state and dimer contribution. This rate can be determined, however, from the rate for the associated spectral change if we assume that it is a parallel process that competes with geminate rebinding, as in the R state. The extrapolated value is virtually the same as is found for the geminate process in the R state, indicating that the low geminate yield in the T state does not arise from an increase in the rate of the competing process, but a marked decrease in the rate of ligand rebinding to the heme [18].

6. Elementary steps in kinetic cooperativity

The difference in affinity of R and T state hemoglobin for carbon monoxide is manifested mainly in the overall association rate [70,76,77]. The R state binds carbon monoxide about 60 -times faster than the T state [18]. In contrast, the overall dissociation rate for the T state is about 10-times faster than that for the R state [78]. The rebinding data in the photolysis experiments can

* An alternative interpretation of the spectral changes in relaxations I–III has been proposed on the basis of a change in the tyrosine resonance Raman spectrum [75]. The observation of a 'T-like' tyrosine spectrum in the deoxy photoproduct of 7 ns laser excitation led to the proposal that the quaternary change occurs in less than 7 ns and that the optical relaxations I–III at 50 ns, 0.5–1 μs, and 20 μs represent the tertiary relaxation in response to the quaternary change. This possibility seems unlikely in view of the observation that relaxation III is absent after photodissociation of the T state, yet relaxations I and II remain in the absence of any possible quaternary change.

be used to explain these differences in the overall rates for the two quaternary structures in terms of the elementary kinetic steps that make up the reaction. To do so we first consider the simplest model that accounts for the major features of the ligand rebinding curve. In this model there are only three significant species for each quaternary structure: the liganded molecule (HbCO), the molecule in which the ligand is dissociated from the heme, but is still localized to the region of the heme pocket (Hb · CO), and the molecule in which the ligand has escaped into the solvent (Hb + CO) [50], i.e.:

$$\underset{\text{Species}}{\overset{1}{\text{HbCO}}} \underset{k_{12}}{\overset{k_{21}}{\rightleftharpoons}} \overset{2}{\text{Hb} \cdot \text{CO}} \underset{k_{23}}{\overset{k_{32}}{\rightleftharpoons}} \overset{3}{\text{Hb} + \text{CO}} \qquad (1)$$

This kinetic scheme introduces the possibility that the quaternary structure can change the overall rate by changing one or more elementary rates (fig. 6).

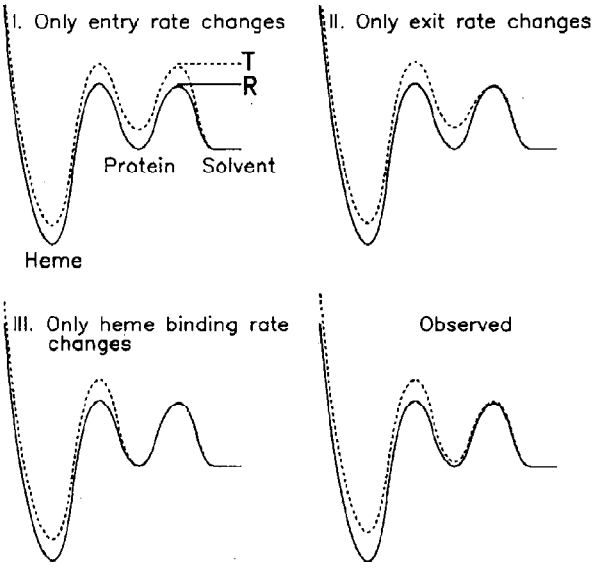

Fig. 6. Schematic diagram for possible origins of kinetic cooperativity (from ref. 18). The relative free energy is plotted vs. the distance between the heme iron and the ligand. The solid curves are for the R state, while the dashed curves are for the T state. Three hypothetical cases are presented in which the decrease by a factor of about 60 in the overall T state binding rate compared to the overall R state binding rate is accomplished by decreasing the rate of entry of the ligand into the protein (case I), increasing the rate of return of the ligand into the solvent (case II), and decreasing the rate of binding to the heme from within the protein (case III). The observed data are very close to case III.

Using the steady-state approximation for the intermediate species (Hb · CO) the relation between the overall dissociation, k_{off}, and association, k_{on}, rates and the kinetic constants of eq. 1 is given by:

$$k_{off} = k_{12}(1-\phi), \quad \phi = k_{21}/(k_{21}+k_{23}),$$
$$k_{gem} = k_{21} + k_{23} \qquad (2)$$

and

$$k_{on} = k_{32}\phi, \qquad (3)$$

where ϕ is the geminate yield and k_{gem} the rate constant for the geminate relaxation phase. For the overall dissociation rate the difference in geminate yields (ϕ) of 0.4 for the R state and < 0.01 for the T state indicates that the heme-ligand bond-breaking rate (k_{12}) is mainly responsible for the difference in factor of 10 for k_{off} [14]. Eq. 2 shows that only a factor of at most 1.7 can be accounted for by the difference in geminate yields for the two quaternary structures.

The geminate process is much more important in determining the difference in overall association rates between the T and R quaternary structures. In considering the association reaction the geminate yield in the photolysis experiments is equivalent to the probability that the ligand will bind to the heme after it enters the protein from the solvent. For the R state the ligand binds to the heme 40% of the time and returns to the solvent 60% of the time. For the T state the probability of binding is less than 1%, and the ligand returns to the solvent over 99% of the time after entering the protein.

The close correspondence between the ratio of the overall association rates (~ 60) and the ratio of the geminate yields (> 40) for the two quaternary structures indicates that the 60-fold slower overall association rate does not arise from a decreased rate of entry (k_{32}) of the ligand from the solvent into the protein in the T state. The decreased overall association rate must result from a low probability of binding to the heme once the ligand has entered the protein. This could in

principle arise either from an increased rate of return of the ligand to the solvent (k_{23}) or a decreased binding rate to the heme (k_{21}) (see eq. 2). The finding that the relaxation time of the associated spectral change ($=1/(k_{21}+k_{23})$) is close to the R state value indicates that the decreased binding rate is responsible [18].

According to the simplest model for the kinetic data, then, it would appear that quaternary structure has little or no effect on the barriers for the entrance and exit of the ligand, but influences the overall association rates almost entirely by changing the rate of binding to the heme from within the protein [18]. Use of a three-species model (eq. 1), however, may be a significant oversimplification. First, we have ignored relaxation II at 0.5–1.0 μs in this analysis. There is very little ligand rebinding in relaxation II, but there is a clear deoxyheme spectral change. This relaxation can be incorporated in a straightforward way by postulating that the ligand does not exit from the protein in relaxation I, but moves from the heme pocket to some other part of the protein. Relaxation II would then correspond to the parallel processes in which the ligand exits from the protein into the solvent, or returns to the heme pocket. In this slightly more complex model, the effect of quaternary structure would still be to alter the rate of binding of the ligand to the heme from within the heme pocket.

In addition to relaxation II, there may be an additional ligand rebinding relaxation occurring on a subnanosecond time scale. As pointed out earlier, transient optical spectra measured with either 8- or 35-ps pulses [3,10,59] show no measurable geminate recombination in less than 10 ns. These experiments were, however, designed for measuring changes in spectral shape, and geminate recombination of less than 10% could have escaped detection. Single-wavelength kinetic studies show that at 10 °C there is about 10% recombination for R state hemoglobin in the time regime 30 ps–2.4 ns [22,79]. Also β^{A} chains in 75% glycerol at room temperature show about 15% geminate recombination with a time constant of approx. 1 ns [80]. There are no data on carbon monoxide rebinding to T state hemoglobin on a subnanosecond time scale, but geminate rebinding cannot be more than a few percent, since the apparent photochemical quantum yield measured with microsecond lasers is greater than 95% [81].

Although the addition of a subnanosecond relaxation and relaxation II would complicate the ligand rebinding mechanism, it does not change the fundamental result that the lower overall association rate for the T state compared to the R state most probably results from a lower rate of binding to the heme from within the protein [18]. It will not be possible to proceed further with the analysis of the mechanism until transient spectra are measured over a wide range of temperatures, as in the single-wavelength studies [80], and the spectra on a subnanosecond time scale are measured with a sensitivity comparable to our nanosecond studies.

7. Origin and significance of the deoxyheme spectral changes

Perhaps the most important question concerning the deoxyheme spectral changes is their functional significance. In the kinetic scheme that we discussed above, it was implicitly assumed that the tertiary conformational changes that produce the deoxyheme spectral changes in relaxations I and II are associated with movement of the ligand from one part of the protein to another or with exit into the solvent. Such a conformational change could result from the collapse of the protein into the 'hole' left by the departing ligand [14]. If these tertiary relaxations are not associated with ligand motion, a more complex model must be employed. The simplest of such models is one in which the photodissociated ligand remains in the heme pocket during relaxation I, and the tertiary conformational change in relaxation I decreases the heme binding rate sufficiently to allow almost all of the remaining unbound ligands to escape into the solvent (or to another part of the protein) [15,34,82,83]. In this model the decreased binding rate at the heme is still responsible for the decreased overall binding rate to the T state. An unattractive feature of this model is that the quaternary structure would have no effect on the rate of the tertiary relaxation that is slowing down the binding rate at the heme.

There are some interesting implications of the model in which the tertiary conformational changes of relaxations I and II have no effect on the binding rate of the ligand to the heme from within the protein. This interpretation requires that if any functionally significant tertiary conformational changes do take place, they must have occurred prior to ligand rebinding, i.e., on a subnanosecond time scale. As pointed out earlier, no such changes have been observed. Both optical absorption [3,10,59] and resonance Raman experiments [27–29,33] have failed to reveal any spectral changes in the time regime 30 ps–10 ns. There are two possible explanations. One is that the protein maintains the conformation of the liganded molecule until relaxation I at 50 ns [34]. In this case the conformational changes of the globin observed by X-ray crystallography [38] would result entirely from ligand motion or escape of the ligand to the solvent during the observed relaxations I and II. The second explanation is that the response of the globin to ligand dissociation is very rapid, occurring in less than 30 ps. Spectral changes due to sub-30-ps conformational changes would be difficult to distinguish from those that result from electronic [2,52,57,58,84] and vibrational relaxation (i.e., heme 'cooling' [43]). In this case some portion of the tertiary conformational changes observed by X-ray crystallography [38] would be associated with the sub-30-ps response to the heme conformational change, and the remainder associated with ligand motion.

The question of the time scale on which functionally significant conformational changes occur relative to that of ligand rebinding is an important issue in interpreting the results at physiological temperatures in terms of the processes observed in low-temperature kinetics. Single-wavelength kinetic studies in the temperature range 100–180 K have been carried out for carbon monoxide rebinding to carp hemoglobin under solvent conditions that favor either the R or T affinity states at room temperature [85]. The nonexponential rebinding was interpreted in terms of an activation energy distribution for rebinding to the heme from within the heme pocket resulting from a distribution of conformational substates that are 'frozen in' at low temperature and bind with different rates [1]. This distribution was then used to calculate the average rate at 280 K, assuming that all conformational substates at this temperature are sampled on a time scale which is short compared to the fastest binding rate. The ratio of the average rates calculated in this way was only 2.5, compared to the ratio of 30 for the overall association rates. From this result the authors concluded that the 'outer barriers' for ligand motion, and not ligand binding at the heme, are being altered by the change in quaternary structure [85]. An alternative explanation for this result is that the distribution of conformational substates at low temperature is the distribution corresponding to the liganded molecules, because at this temperature protein conformational changes that affect the binding rate have not yet occurred (these would presumably correspond to the sub-30-ps conformational changes that may occur in human hemoglobin at room temperature).

Up to now we have only presented a phenomenological discussion of the deoxyheme spectral changes, with no attempt to give any detailed structural interpretation. The reason is simply that the optical spectra of deoxyhemes are complex [41,46] and not sufficiently well understood to provide any concrete theoretical insights. However, it is clearly important to understand the structural origin of changes in the heme optical spectrum in order to incorporate the results of X-ray crystallography into the binding mechanism. A brief discussion is therefore worthwhile at this point in order to clarify the principal issues.

All of the optical changes that have been observed up to now appear to be exclusively associated with the deoxyhemes (figs. 4 and 5). No changes in the spectrum of the heme-CO complex have been observed, either because they are fast relative to the ligand rebinding rates, or because the spectrum is relatively insensitive to conformational changes [36,86]. One of the major findings concerning the deoxyheme spectral changes is that they all have very similar shapes (figs. 4 and 5), suggesting that the structural changes responsible for the spectral changes are very similar. Also, the amplitudes for the tertiary conformational changes are very similar in magnitude for the R and T quaternary structures. After normalizing for the

number of deoxyhemes that undergo the R → T transition, the amplitude of the quaternary transition is larger than the sum of the amplitudes for the two tertiary changes. This is consistent with the finding from X-ray crystallography that conformational changes associated with the quaternary change are larger than the tertiary conformational changes upon ligand dissociation within either the R or T quaternary structure [38].

The tertiary conformational changes observed crystallographically are different for the R and T quaternary structures [38], suggesting that the changes in the optical spectra do not arise solely from changes in the heme environment. A more likely cause for the optical spectral changes is that the globin conformational change is coupled to a change in the geometry of the heme complex. Several changes in the geometry of the heme complex are known from X-ray crystallography to occur upon ligand dissociation within the R or T quaternary structures, or upon switching from the deoxy R to deoxy T quaternary structure. These include displacement of the iron from the heme plane toward the proximal histidine, tilting of the histidine imidazole ring relative to the porphyrin plane, and doming of the porphyrin ring [38]. The most likely candidate for the origin of the observed spectral changes is the iron displacement, since it is the only change that appears to be clearly common to the three types of conformational changes examined in the time-resolved optical experiments (i.e., tertiary conformational changes resulting from ligand dissociation within the R or T quaternary structures, and tertiary conformational changes resulting from the switch from deoxy R to deoxy T) [38].

Since the d-orbital energy levels are sensitive to the detailed geometry of the iron-ligand complex, changes in the iron position could have an indirect effect on the Soret $\pi \rightarrow \pi^*$ transition as a result of changes in the population of the sublevels of the ground electronic state. * A more direct effect would be expected on transitions in which the d-orbitals are directly involved in the optical transition. Such an effect has been observed on the 760 nm charge-transfer band [26,88,89] which arises from the orbital promotion: porphyrin, $a_{2u}(\pi) \rightarrow$ iron, d_{yz} [46]. **. The band of the immediate photoproduct is initially red-shifted compared to the equilibrium spectrum, and moves toward the equilibrium spectrum as a function of time with kinetics at room temperature that are very similar, and possibly identical, to what is observed for the Soret band [26]. The blue shift with time is consistent with the results of extended Hückel calculations on the imidazole complex of ferrous porphin (L.K. Hanson and W.A. Eaton, unpublished results). These calculations show that the energy of the iron d_{yz} orbital increases with

* The spectral change of the Soret band of the deoxyheme photoproduct is mainly an increase in intensity and a slight blue shift with increasing time (figs. 4 and 5). The ground electronic state of deoxyheme has the d-electron configuration $d_{xz}^2 d_{xy} d_{yz} d_{z^2} d_{x^2-y^2}$ [46,49], which derives from a state in octahedral symmetry that is 15-fold degenerate ($^5T_2$). Although the 3-fold orbital degeneracy is removed by the asymmetric ligand field of the pyrrole nitrogens and proximal histidine, and the 5-fold spin degeneracy by spin-orbit coupling, 11 sublevels are spread over an energy range of only 400 cm^{-1} [49]. One of these derives from the $^1A_1$ state with the low-spin configuration $d_{xz}^2 d_{xy}^2 d_{yz}^2$, and is calculated to lie about 100 cm^{-1} above the lowest sublevel. The low energy of the separation between these 11 sublevels suggests that rather small structural changes could produce significant changes in their relative population. Differences in the wave functions for the individual sublevels could result in different transition intensities. The biggest difference would be expected for transitions from the $^1A_1$ state, which would also be expected at different energy. Changes in the population of this singlet state are analogous to the high-spin, low-spin equilibrium observed in ferric heme proteins, where there are large optical changes [87].

** An alternative assignment for the 760 nm band has been proposed in which the orbital promotion responsible for the transition is iron, $d_{x^2-y^2} \rightarrow$ porphyrin, $e_g(\pi^*)$ [90]. Because of the degeneracy of the acceptor orbital in the electronic promotion this assignment predicts that the transition exhibit x,y-polarization. A careful determination of the polarization for the 760 nm band of the deoxyhemoglobin single crystal shows that it is not x,y but is consistent with the nondegenerate porphyrin, $a_{2u}(\pi) \rightarrow$ iron, d_{yz} [46]. For deoxymyoglobin the polarization was reported as x,y [90], but this conclusion was based on an indirect procedure [91] in which the contribution from the 760 nm band to the crystal polarization ratio in this wavelength region was not separately determined. The $d_{x^2-y^2} \rightarrow e_g(\pi^*)$ assignment is also inconsistent with the observation of very weak natural circular dichroism, since this transition should have significant magnetic dipole strength [41,46,92,93].

increasing displacement of the iron from the porphin plane, with no significant change in the energy of the porphryin $a_{2u}(\pi)$ orbital. It would be worthwhile at this point to carry out more realistic calculations of the spectra of deoxyhemes as a function of geometry to test these ideas, and to explore other possible causes for the optical changes, such as changes in the tilt of the proximal histidine with respect to the heme plane [34], and changes in porphyrin doming.

Acknowledgement

We thank Attila Szabo for many helpful discussions of this work.

References

1 R.H. Austin, K.W. Beeson, L. Eisenstein, H. Frauenfelder and I.C. Gunsalus, Biochemistry 14 (1975) 5355.
2 C.V. Shank, E.P. Ippen and R. Bersohn, Science 193 (1976) 50.
3 B.I. Greene, R.M. Hochstrasser, R.B. Weisman and W.A. Eaton, Proc. Natl. Acad. Sci. U.S.A. 75 (1978) 5255.
4 L.J. Noe, W.G. Eisert and P.M. Rentzepis, Proc. Natl. Acad. Sci. U.S.A. 75 (1978) 573.
5 D.A. Duddell, R.J. Morris and J.T. Richards, J. Chem. Soc. Chem. Commun. (1979) 75.
6 B. Alpert, S. El Mohsni, L. Lindqvist and F. Tfibel, Chem. Phys. Lett. 64 (1979) 11.
7 J.M. Friedman and K.B. Lyons, Nature 284 (1980) 570.
8 D.A. Duddell, R.J. Morris, N.J. Muttucumaru and J.T. Richards, Photochem. Photobiol. 31 (1980) 479.
9 D.A. Duddell, R.J. Morris and J.T. Richards, Biochim. Biophys. Acta 621 (1980) 1.
10 D.A. Chernoff, R.M. Hochstrasser and A.W. Steele, Proc. Natl. Acad. Sci. U.S.A. 77 (1980) 5606.
11 L. Lindqvist, S. El Mohsni, F. Tfibel, B. Alpert and J.C. Andre, Chem. Phys. Lett. 79 (1981) 525.
12 R.J. Morris, D.A. Duddell and J.T. Richards, in: Hemoglobin and oxygen rebinding, ed. C. Ho (Elsevier/North-Holland, New York, 1982) p. 339.
13 R. Catterall, D.A. Duddell, R.J. Morris and J.T. Richards, Biochim. Biophys. Acta 705 (1982) 257.
14 J. Hofrichter, J.H. Sommer, E.R. Henry and W.A. Eaton, Proc. Natl. Acad. Sci. U.S.A. 80 (1983) 2235.
15 J. Hofrichter, E.R. Henry, J.H. Sommer, R. Deutsch, M. Ikeda-Saito, T. Yonetani and W.A. Eaton, Biochemistry 24 (1985) 2667.
16 B.F. Campbell, D. Magde and V.S. Sharma, J. Biol. Chem. 260 (1985) 2752.
17 S. Pin, P. Valat, H. Tourbez and B. Alpert, Chem. Phys. Lett. 128 (1986) 79.
18 L.P. Murray, J. Hofrichter, E.R. Henry, M. Ikeda-Saito, K. Kitagishi, T. Yonetani and W.A. Eaton, Proc. Natl. Acad. Sci. USA (1987) in the press.
19 R.J. Morris, Q.H. Gibson, M. Ikeda-Saito and T. Yonetani, J. Biol. Chem. 259 (1984) 6701.
20 Q.H. Gibson, M. Ikeda-Saito and T. Yonetani, J. Biol. Chem. 260 (1985) 14126.
21 P. Valat, H. Tourbez and B. Alpert, Laser Chem. 1 (1982) 45.
22 J.M. Friedman, T.W. Scott, G.J. Fisanick, S.R. Simon, E.W. Findsen, M.R. Ondrias and V.W. MacDonald, Science 229 (1985) 187.
23 M.F. Perutz and F.S. Mathews, J. Mol. Biol. 21 (1966) 199.
24 C.L. Nobbs, in: Hemes and hemoproteins, eds. B. Chance, R.W. Estabrook and T. Yonetani (Academic Press, New York, 1966) p. 143.
25 L. Lindqvist, S. El Mohsni, F. Tfibel and B. Alpert, Nature 288 (1980) 729.
26 M. Sassaroli and D.L. Rousseau, Biochemistry 26 (1987) 3092.
27 J. Terner, T.G. Spiro, M. Nagumo, M.F. Nicol and M.A. El-Sayed, J. Am. Chem. Soc. 102 (1980) 3238.
28 J. Terner, J.D. Stong, T.G. Spiro, M. Nagumo, M. Nicol and M.A. El-Sayed, Proc. Natl. Acad. Sci. U.S.A. 78 (1981) 1313.
29 P. Stein, J. Terner and T.G. Spiro, J. Phys. Chem. 86 (1982) 168.
30 K.B. Lyons and J.M. Friedman, in: Hemoglobin and oxygen rebinding, eds. C. Ho, W.A. Eaton, J.P. Collman, Q.H. Gibson, J.S. Leigh, E. Margoliash, K. Moffat and W.R. Scheidt (Elsevier/North-Holland, New York, 1982) p. 333.
31 J.M. Friedman, T.W. Scott, R.A. Stepnoski, M. Ikeda-Saito and T. Yonetani, J. Biol. Chem. 258 (1983) 10564.
32 T.W. Scott and J.M. Friedman, J. Am. Chem. Soc. 106 (1984) 5677.
33 E.W. Findsen, J.M. Friedman, M.R. Ondrias and S.R. Simon, Science 229 (1985) 661.
34 J.M. Friedman, Science 228 (1985) 1273.
35 M.F. Perutz, Nature 228 (1970) 726.
36 M.F. Perutz, J.E. Ladner, S.R. Simon and C. Ho, Biochemistry 13 (1974) 2163.
37 J. Baldwin and C. Chothia, J. Mol. Biol. 129 (1979) 175.
38 M.F. Perutz, G. Fermi, B. Luisi, B. Shaanan and R.C. Liddington, Acc. Chem. Res. 20 (1987) 309.
39 M.W. Makinen and W.A. Eaton, Nature 247 (1974) 62.
40 J. Hofrichter and W.A. Eaton, Annu Rev. Biophys. Bioeng. 5 (1976) 511.
41 W.A. Eaton and J. Hofrichter, Methods Enzymol. 76 (1981) 175.
42 E.R. Henry, M. Levitt and W.A. Eaton, Proc. Natl. Acad. Sci. U.S.A. 82 (1985) 2034.
43 E.R. Henry, W.A. Eaton and R.M. Hochstrasser, Proc. Natl. Acad. Sci. U.S.A. 83 (1986) 8982.
44 E.R. Henry, J. Hofrichter, J.H. Sommer and W.A. Eaton, in: Photochemistry and photobiology, ed. A.H. Zewail (Harwood Academic, New York, 1983) p. 791.
45 M.W. Makinen and W.A. Eaton, Ann. N.Y. Acad. Sci. 206 (1973) 210.

46 W.A. Eaton, L.K. Hanson, P.J. Stevens, J.C. Sutherland and J.B.R. Dunn, J. Am. Chem. Soc. 100 (1978) 4991.
47 M. Zerner, M. Gouterman and H. Kobayashi, Theor. Chim. Acta 6 (1966) 363.
48 A. Waleh and G.H. Loew, J. Am. Chem. Soc. 104 (1982) 2346.
49 H. Eicher, D. Bade and F. Parak, J. Chem. Phys. 64 (1976) 1446.
50 E.R. Henry, J.H. Sommer, J. Hofrichter and W.A. Eaton, J. Mol. Biol. 166 (1983) 443.
51 J.L. Martin, A. Migus, C. Poyart, Y. Lecarpenter, R. Astier and A. Antonetti, Proc. Natl. Acad. Sci. U.S.A. 80 (1983) 173.
52 J.L. Martin, A. Migus, C. Poyart, Y. Lecarpenter, R. Astier and A. Antonetti, in: Ultrafast phenomena IV, eds. D.H. Ausyin and K.B. Eisenthal (Springer-Verlag, New York, 1984) p. 447.
53 S. Dasgupta and T.G. Spiro, Biochemistry 25 (1986) 5941.
54 S.A. Asher and J. Murtaugh, J. Am. Chem. Soc. 105 (1983) 7244.
55 B.R. Brooks and M. Karplus, Proc. Natl. Acad. Sci. U.S.A. 80 (1983) 6571.
56 M. Levitt, C. Sander and P.S. Stern, J. Mol. Biol. 181 (1985) 423.
57 P.A. Cornelius, A.W. Steele, D.A. Chernoff and R.M. Hochstrasser, Proc. Natl. Acad. Sci. U.S.A. 78 (1981) 7526.
58 J.A. Hutchinson and L.J. Noe, IEEE J. Quantum Electron. QE-20 (1984) 1353.
59 S.M. Janes, G.A. Dalickas, W.A. Eaton, and R.M. Hochstrasser, Biophys. J. (1987) submitted for publication.
60 J. Monod, J. Wyman and J.-P. Changeux, J. Mol. Biol. 12 (1965) 88.
61 J.J. Hopfield, R.G. Shulman and S. Ogawa, J. Mol. Biol. 61 (1971) 425.
62 A. Szabo and M. Karplus, J. Mol. Biol. 72 (1972) 163.
63 R.G. Shulman, J.J. Hopfield and S. Ogawa, Q. Rev. Biophys. 8 (1975) 325.
64 M. Ikeda-Saito, H. Yamamoto, K. Imai, F.J. Kayne and T. Yonetani, J. Biol. Chem. 252 (1977) 620.
65 M. Ikeda-Saito and T. Yonetani, J. Mol. Biol. 138 (1980) 845.
66 T.W. Scott, J.M. Friedman, M. Ikeda-Saito and T. Yonetani, FEBS Lett. 158 (1983) 68.
67 G. Fermi, M.F. Perutz, L.C. Dickinson and J.C.W. Chien, J. Mol. Biol. 155 (1982) 495.
68 K. Imai, T. Yonetani and M. Ikeda-Saito, J. Mol. Biol. 109 (1977) 83.
69 G.H. Golub and C. Reinsch, Numer. Math. 14 (1970) 403.
70 C.A. Sawicki and Q.H. Gibson, J. Biol. Chem. 251 (1976) 1533.
71 G.K. Ackers and M.L. Johnson, J. Mol. Biol. 147 (1981) 559.
72 S.J. Edelstein and J.T. Edsall, Proc. Natl. Acad. Sci. U.S.A. 83 (1986) 3796.
73 A. Arnone and M.F. Perutz, Nature 249 (1974) 34.
74 M.F. Perutz, G. Fermi, D.J. Abraham, C. Poyart and E. Bursaux, J. Am. Chem. Soc. 108 (1986) 1064.
75 S. Dasgupta, R.A. Copeland and T.G. Spiro, J. Biol. Chem. 261 (1986) 10960.
76 A. Szabo, Proc. Natl. Acad. Sci. U.S.A. 75 (1978) 2108.
77 J.S. Olson, Methods Enzymol. 76 (1981) 631.
78 V.S. Sharma, M.R. Schmidt and H.M. Ranney, J. Biol. Chem. 251 (1976) 4267.
79 T.W. Scott, J.M. Friedman and V.W. MacDonald, J. Am. Chem. Soc. 107 (1985) 3702.
80 A. Ansari, E.E. DiIorio, D.D. Dlott, H. Frauenfelder, I.E.T. Iben, P. Langer, H. Roder, T.B. Sauke and E. Shyamsunder, Biochemistry 25 (1986) 3139.
81 C.A. Sawicki and Q.H. Gibson, J. Biol. Chem. 254 (1979) 4058.
82 E.R. Henry, J. Hofrichter, J.H. Sommer and W.A. Eaton, in: Hemoglobins: structure and function, eds. A.G. Schnek and C. Paul (Brussels University Press, Brussels, 1983) p. 193.
83 N. Agmon and J.J. Hopfield, J. Chem. Phys. 79 (1983) 2042.
84 K. Caldwell, L.J. Noe, J.D. Ciccone and T.G. Traylor, J. Am. Chem. Soc. 108 (1986) 6150.
85 W.G. Cobau, J.D. LeGrange and R.H. Austin, Biophys. J. 47 (1985) 781.
86 M.F. Perutz, J.V. Kilmartin, K. Nagai, A. Szabo and S.R. Simon, Biochemistry 15 (1976) 378.
87 P. George, J. Beetlestone and J.S. Griffith, in: Haematin enzymes, eds. J.E. Falk, R. Lemberg and R.K. Morton (Pergamon Press, Oxford, 1961) p. 105.
88 T. Iizuka, H. Yamamoto, M. Kotani and T. Yonetani, Biochim. Biophys. Acta 371 (1974) 126.
89 A. Ansari, J. Berendzen, S.F. Bowne, H. Frauenfelder, I.E.T. Iben, T.B. Sauke, E. Shyamsunder and R.D. Young, Proc. Natl. Acad. Sci. U.S.A. 82 (1985) 5000.
90 M.W. Makinen and A.K. Churg, in: Iron porphyrins, eds. A.B.P. Lever and H.B. Gray (Addison-Wesley, Reading, MA, 1983) part I, p. 141.
91 A.K. Churg and M.W. Makinen, J. Chem. Phys. 69 (1978) 1913. Erratum, J. Chem. Phys. 68 (1978) 2268.
92 W.A. Eaton and E. Charney, J. Chem. Phys. 51 (1969) 4502.
93 W.A. Eaton and E. Charney, in: Probes of structure and function of macromolecules and membranes, eds. B. Chance, C.P. Lee and J.K. Blasie (Academic Press, New York, 1971) vol. 1, p. 155.